Identification of a heat source model for multipass narrow groove GMA welding process

Olivier Asserin, Danièle Ayrault, Philippe Gilles, Evelyne Guyot, Jeanne Schroeder

Identification of a heat source model for multipass narrow groove GMA welding process

Olivier Asserin, Danièle Ayrault, Philippe Gilles, Evelyne Guyot & Jeanne Schroeder

Welding in the World
The International Journal of Materials Joining

ISSN 0043-2288

Weld World
DOI 10.1007/s40194-013-0109-4

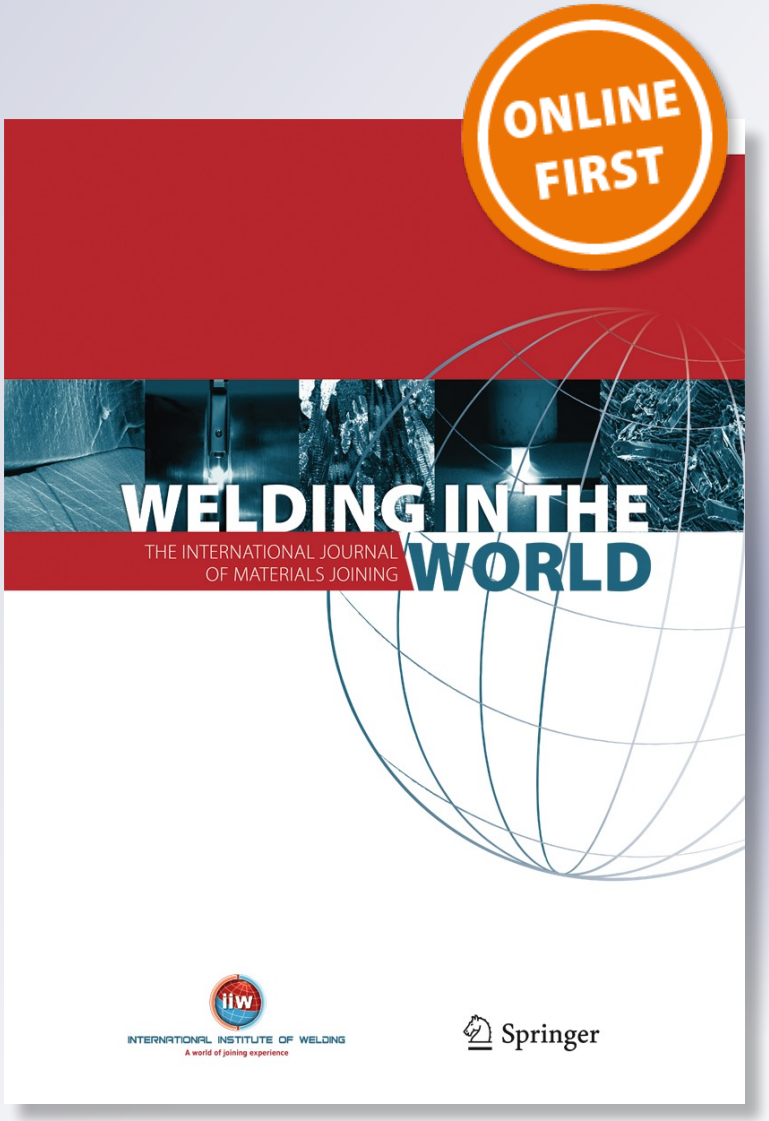

Springer

Weld World
DOI 10.1007/s40194-013-0109-4

RESEARCH PAPER

Identification of a heat source model for multipass narrow groove GMA welding process

Olivier Asserin · Danièle Ayrault · Philippe Gilles · Evelyne Guyot · Jeanne Schroeder

Received: 14 March 2013 / Accepted: 17 October 2013

Abstract The use of narrow gap for thick component welding as applied in nuclear industries and especially by AREVA NP, requires the mastering of several parameters and especially shrinkage. The prediction through to numerical simulation is very helpful for welding procedure definition. This paper describes an approach used to determine a 3D heat source dedicated to a new industrial welding process configuration (deep narrow groove multipass low-carbon steel gas metal arc (GMA) welding, two passes per layer) to assess the groove shrinkage which occurs during welding by numerical simulation. Parameters of this 3D heat source are identified by solving an inverse heat conduction problem by a least square method. A multiobjective optimization is performed with a new proposed metric (*Hausdorff* distance) in the objective function (sum of square) in order to simulate relevant bead shape and temperatures in the solid zone. Finally, the identified 3D heat source model is a combination of two volumetric heat sources containing five parameters each. It can be used as thermal loading for subsequent thermal metallurgical mechanical calculations.

Doc. IIW-2425, recommended for publication by Commission XII "Arc Welding Processes and Production Systems".

O. Asserin (✉) · D. Ayrault
CEA, DEN, DM2S,
91191 Gif-sur-Yvette, France
e-mail: olivier.asserin@cea.fr

P. Gilles
AREVA NP, Tour AREVA, 1 place Jean Millier,
92400 Courbevoie, France

E. Guyot · J. Schroeder
AREVA NP, Technical Center, BP 40001 Saint Marcel,
71328 Chalon sur Saône, France

Keywords Narrow gap welding · GMA welding · Simulating · Heat flow · Process procedures · Optimization

1 Introduction

Nuclear components require welds of perfect and reproducible quality. Moreover, for a given welding process, productivity requirements also lead to reduce the volume of deposited metal and thus to use narrow gap design. With this technology, the definition of the groove geometry is a very important step. The shrinkage that occurs during the filling has to be foreseen and integrated into the groove dimensions. In order to facilitate groove definition and welding procedure establishment, AREVA NP has developed a practical numerical tool dedicated to narrow groove. This tool allows calculating for orbital welding the shrinkage with automatic meshing and thermal calculation. This tool has been validated for deep narrow groove gas tungsten arc welding (GTAW) process, and one objective is now to add other used processes as gas metal arc welding (GMAW). Within this framework, the key element is the definition of the appropriate heat source and its calibration in the thermal modeling. The main objective of this work is to identify, by inverse method, a 3D thermal model for a deep narrow groove multipass low-carbon steel GMAW process configuration. The challenge is to determine a relevant thermal load for a reliable thermomechanical simulation and especially shrinkage prediction.

The methodology is based on an experimental and numerical coupled approach. Considering one welding configuration (process, geometry), the heat transferred into the workpiece is modeled as an apparent (equivalent) welding heat source [1]. This heat source is represented by a mathematical model of the heat distribution within a

Published online: 08 November 2013

finite region of the material. The parameters of the model are identified, thanks to the resolution of an inverse heat conduction problem consisting in minimizing difference between calculation and experience. The observable parameters are temperatures close to the weld pool region and the bead shape dimensions. In the following paragraphs, the thermal instrumentation and profile acquisition as well as the welded mock-up welding are presented. Then the numerical calculation and the proposed thermal model are introduced.

2 Experimental setup and data analysis

The calibration of the thermal model requires temperature measurements as accurate as possible with a precise location and in the hottest zones close to the fusion line. The sensors must have a limited intrusive effect in order not to disturb the thermal phenomena linked to welding. Thus, a specific, very fine instrumentation method has been developed.

To validate the thermal and mechanical simulation, we used a noncontact laser system to measure geometrical data during welding. Those data are the position and shape (profile) of each bead inside the groove and the width of the groove evolution. This section presents the different types of instrumentation, mock-up welding conditions, and type of measurements.

2.1 Mock-up manufacturing and welding

The mock-up is machined in an AFNOR 16MND5 steel representative of nuclear materials for pressure vessel: 600 mm long, 350 mm wide, and 90 mm thick. The groove is 12 mm wide at the top surface and 80 mm deep, and the included angle is about 1°. The plate has been cut into four blocks; two surfaces have been instrumented with 27 thermocouples on each—14 on one side of the groove and 13 on the other side (Figs. 1 and 2). The mock-up has been rebuilt with a GTAW with filler wire in order to insure the contact between the blocks. To increase the stiffness, transverse metal rods have been inserted all along the mock-up (Fig. 1). In addition, new stiffeners have been welded at the mock-up back side.

2.2 Methodology for thermal instrumentation

The thermal instrumentation is conducted in three steps: first, the mock-up is cut into four parts perpendicularly to the welding axis (Fig. 1), the thermocouples are inserted on two surfaces (see Fig. 2), and finally, the four parts of the mock-up are welded together (closing welding). Very thin K type thermocouples (50 μm in diameter) are chosen for their instantaneous response. They are welded at the flat

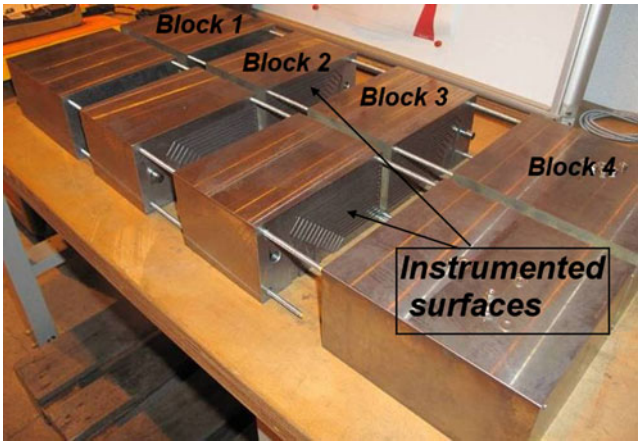

Fig. 1 Four blocks constituting the mock-up with metallic rods as stiffeners

bottom of a hole 0.6 mm in diameter and 1 mm in depth oriented parallel to the welding axis. The orientation of the thermocouples is chosen to be parallel to an isotherm, in order to limit the measurements errors. This operation is carried out using a micro-capacitor electrical discharge device especially developed for this application. The thermocouple wires are then routed in transverse grooves to the welding axis filled with thermal glue up to the exit at the rear part of the mock-up. Then they are connected to a recorder. The optimal location of the thermocouples was defined on the basis of preliminary mock-up measurements and computations following an optimal design experiment process [2–4].

After the installation of the mock-up and the preheating system, the 54 thermocouples were connected to an acquisition system (Fig. 3). In addition to the temperature measurement, amperage and voltage are also recorded in a synchronized way. Two data acquisition systems were used:

– subframe SCXI, for thermocouples and amperage with an acquisition frequency of 500 Hz,

Fig. 2 Thermocouple location at one block surface

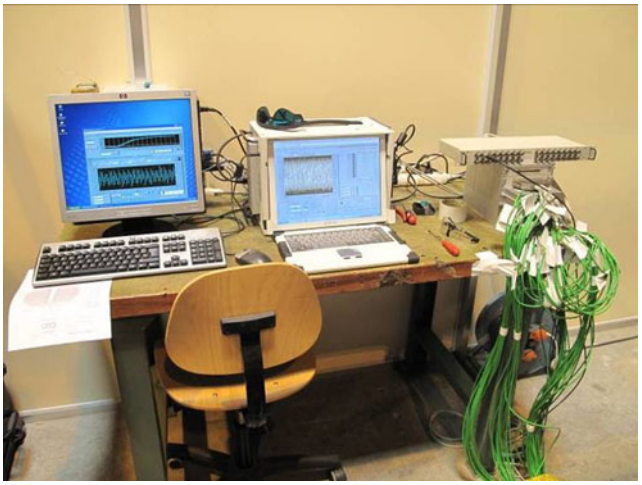

Fig. 3 Temperature, amperage, and voltage acquisition setup

– subframe PXI, for amperage and voltage with an acquisition frequency 10,000 Hz.

The mock-up has been welded with GMAW in two beads per layer (25 passes). The average welding parameters are presented in Table 1. The general conditions are flat position welding, Bohler Thyssen Union I Mo Mn (Ø1.2 mm) filler wire, preheating between 125 and 225 °C. This process is used for the final weld of bi-block steam generator replacement.

2.3 Profile acquisition

In order to measure the profile of each bead, a laser profilometer (DLS 200 from Metavision) has been installed (Fig. 4). The plotting is done during the way back of the head. An algorithm developed by AREVA NP allows to cumulate the profiles and to rebuild the complete multipass weld (Fig. 4). From those data, the pass thickness or the geometry of the bead surface can be evaluated.

2.4 Bead shape and thermocouples position

After welding, macrographs have been made in order to extract the bead shape and an exact location of the thermocouples. Those informations are helpful to calibrate the heat source model and to improve meshing definition. The knowledge on thermocouple locations relatively to the bead is necessary to increase the validity of the comparison between calculation and experimental temperature values. The location of the thermocouples on the macrograph, the cross section of the beads, and the bead shape are illustrated on the Fig. 5.

Table 1 Average welding conditions

Amperage (A)	Voltage (V)	Welding speed (cm min^{-1})	Wire speed (m min^{-1})
300	30	35	12

2.5 Measured temperatures

All the thermocouples have worked properly; temperatures above 1,000 °C were measured that demonstrates the quality of the instrumentation. A data posttreatment was required to reduce the data quantity: sampling reduction to 20 Hz, temporal adjustment, and selections of the thermocouples that have exceeded 300 °C. An example of obtained temperature curves is given in Fig. 5 for the 13th pass.

3 Numerical simulation in the moving frame

3.1 Methodology

The heat source model has been identified by means of a numerical tool called WPROCESS and developed by the CEA (French Alternative Energies and Atomic Energy Commission). The long-term objective of this tool is to propose a direct and predictive simulation of the welding process based on multiphysical modeling (arc, weld pool, and coupling). At the present time, WPROCESS includes an operational unit which allows proposing a thermal model for the considered welding configuration by inverse analysis, without modeling the complex physical phenomena. This approach consists in using a simplification to describe the heat transfer during welding, considering the equivalent heat source concept which produces the required weld pool geometry and consequently the adequate temperature field in the solid zone. The heat source model is then described by a mathematical model of the heat distribution depending on unknown parameters which are estimated by the resolution of an inverse heat conduction problem, from experimental welding data (temperatures and bead shape). WPROCESS used the CEA finite elements code Cast3M (http://www-cast3m.cea.fr) and the Salome platform (http://www.salome-platform.org). In the WPROCESS tool, the dimensions of the plate, the groove geometry, and the deposits geometry can be changed. Meshing is also parameterized, and it is possible to refine it in regions of interest as, for example, the instrumented area with thermocouples. The global methodology which is implemented in WPROCESS [4] to identify a thermal heat source model consists in a first step in proposing the models supposed to describe adequately the heat transfer during welding for the considered configuration. After that, a sensitivity analysis indicates the models which can be retained for a relevant estimation of their parameters. Then, a design of optimum experiment is

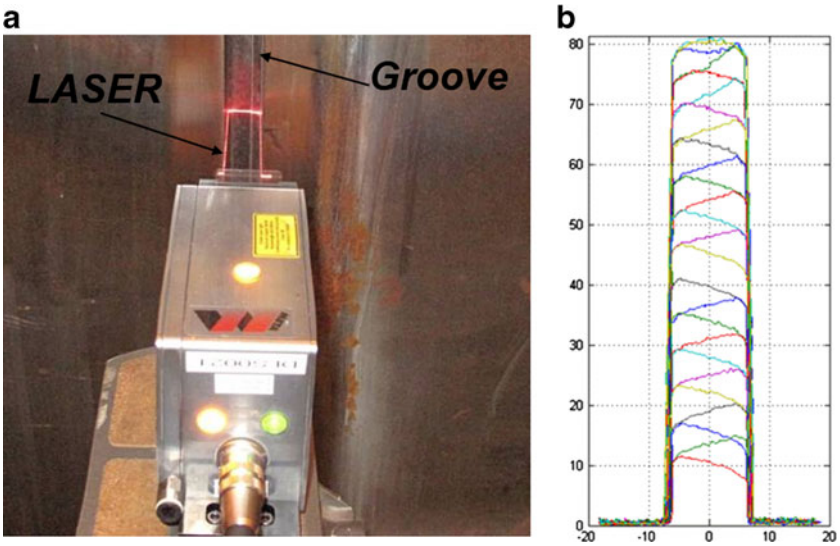

Fig. 4 Laser profilometer system (**a**) and measured (millimeter) bead profiles (**b**)

carried out in order to determine the number of thermal sensors and their location which will be used for the instrumentation. Finally, the heat source can be calibrated from these experimental data by inverse analysis.

3.2 Thermal model

3.2.1 General conditions for direct calculations of temperature field

The thermal problem is solved in a moving coordinate system; a heat transfer quasi-steady state can be achieved in a coordinate system that moves with the heat source. It means that the size of the weld pool and the temperature field in the solid domain are constant. The model is 3D, and thermal properties are nonlinear (temperature-dependent). The governing Eq. 1 is solved to calculate the temperature field:

$$\rho(T)C(T)\nabla.\boldsymbol{u}T = \lambda(T)\Delta T + q_{\text{app}} \tag{1}$$

In Eq. 1, ρ represents the density (kilograms per cubic meter), C is the specific heat (joules per kilogram per kelvin), T is the temperature field (kelvin), u is the torch

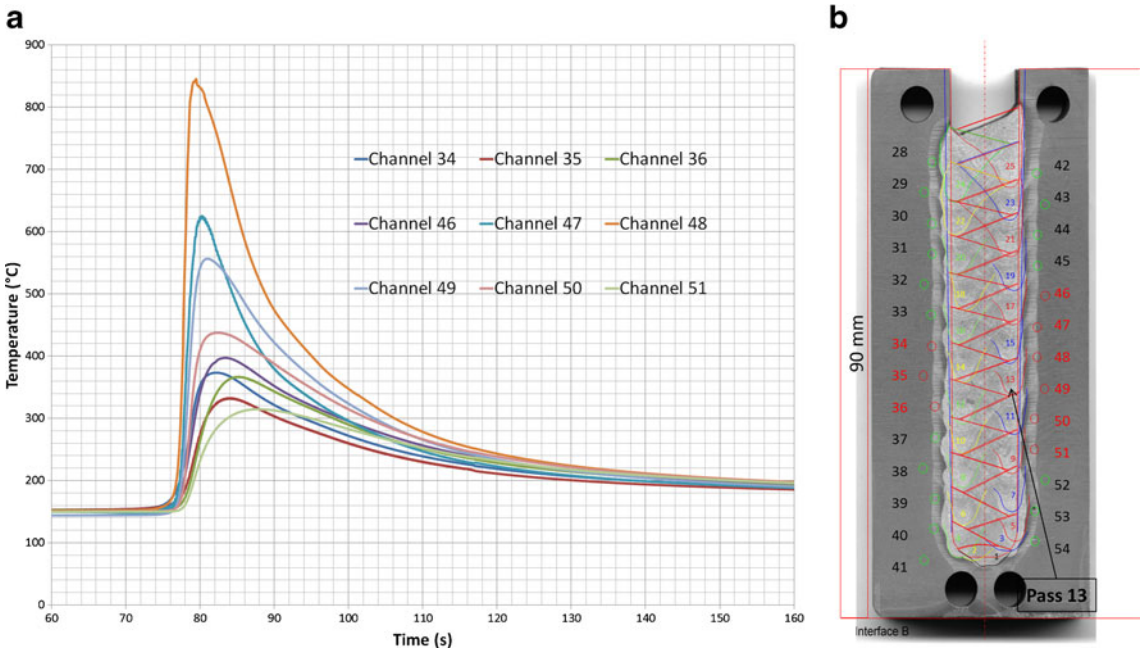

Fig. 5 Measured temperatures for pass 13 (**a**) and cross-section macrograph with thermocouple location (*circle marker*) (**b**)

velocity (meters per second), λ is the thermal conductivity (watts per meter per kelvin), and q_{app} is an apparent volumic heat source density (watts per cubic meter) corresponding to the transferred welding volumic energy density into the workpiece. Different boundary conditions are applied to the system such as a prescribed preheating temperature and radiative and convective heat losses [1] applied to the top, bottom, and lateral surfaces of the welded specimen. The simulated configuration is the same as the experimental welding specimen described in Section 2 consisting in the GMAW of a thick plate with a narrow groove. The WPROCESS tool is used to identify the heat source model.

3.2.2 Heat source model for narrow gap GMAW

Analytical method [5] to simulate the thermal process is not applicable with regards to the special shape of our bead. Integrated approach based on the use of design of experiment, artificial neural networks, and genetic algorithm [6] is not useful in our case because we cannot make several experiment. Other authors [7, 8] consider fluid flows in the weld pool but only for elementary configuration. Previous studies on narrow gap gas tungsten arc multipass welding [9–11] have shown that the heat transfer is well described by the *Goldak* double ellipsoidal model [1] which distinguishes energy distributions on the torch front and the rear and considers only the heat transfer by conduction in the solid part of the workpiece. In the torch frame, the mathematical relations for this heat source are as follows:

$$\left\{\begin{array}{l} q_f(x,y,z) = Qf_f \dfrac{6\sqrt{3}}{abc_f\pi\sqrt{\pi}} \exp\left(-3\left(\left(\frac{x}{c_f}\right)^2 + \left(\frac{y}{a}\right)^2 + \left(\frac{z}{b}\right)^2\right)\right) \\ q_r(x,y,z) = Qf_r \dfrac{6\sqrt{3}}{abc_r\pi\sqrt{\pi}} \exp\left(-3\left(\left(\frac{x}{c_r}\right)^2 + \left(\frac{y}{a}\right)^2 + \left(\frac{z}{b}\right)^2\right)\right) \\ f_f + f_r = 2 \end{array}\right\} \tag{2}$$

Where x, y, z are the coordinate of a solid point in the moving frame; c_f is the length of the half ellipsoid along x-axis on the front of the torch (along the weld path); c_r is the length of the half-ellipsoid along the x-axis on the rear of the torch; Q is the transfered energy into the workpiece; a the width of the half-ellipsoid along y-axis (transverse to the weld path); b the depth of the half-ellipsoid along z-axis; and f_f and f_r are the front and the rear energy distribution fraction, respectively. Thus, this model contains five independent unknown parameters (c_f, c_r, a, b, Q).

In the present case, there are two deposits by layer, and the bead shape is asymmetric (Fig. 5); therefore, we considered that the welding process can be modeled by a combination of two *Goldak* volumetric heat sources as it appears in Fig. 6.

3.2.3 Heat source sensitivity analysis

A sensitivity analysis of this combined heat sources has been carried out to ensure that each of the unknown parameters of the heat source-combined model can be identified. Considering the temperature (T) as the output of the model, the sensitivity coefficient X is calculated for each parameter β as the following (Eq. 3):

$$X = \frac{\partial T(\beta)}{\partial \beta} \tag{3}$$

This quantity is approximated using the centered finite difference method (4). $\Delta\beta$ represents a relative variation of parameter β of about $\pm 10^{-3}$.

$$X = \frac{\partial T(\beta)}{\partial \beta} \approx \frac{T(\beta + \Delta\beta) - T(\beta - \Delta\beta)}{2\Delta\beta} \tag{4}$$

An important absolute value of the sensitivity coefficient means that the model presents a sensitivity to the considered parameter. Because all the parameters do not have the same dimensions, to make possible the comparison of the parameters sensitivity, a reduced sensitivity coefficient $\bar{X}_j$ is used (Eq. 5).

$$\bar{X} = \beta \frac{\partial T(\beta)}{\partial \beta} \tag{5}$$

Some examples of reduced sensitivity coefficient field in the moving frame are given on Figs. 7 and 8, for the *Goldak* in the left side of the groove (the biggest one). On those figures, only a focus of the left side of the groove is shown. Important differences appear between the parameters. The parameter Q is the more sensitive parameter about 500 °C at maximum, an increase of Q will increase the size of weld pool. Considering a parameter, an increase of it will increase the width of weld pool and decrease the length and depth. This parameter is also very sensitive with a maximum sensitivity about one half of those of Q (246 °C). An increase of b parameter will increase the depth of weld pool and decrease the length and width; the maximum sensitivity is much more than a but less than those of Q with 389 °C. For c_f and c_r, the maximum sensitivity is less than 100 °C, and an increase of c_f will increase the size of the front part of weld pool and decrease the rear part—this is the inverse for c_r, respectively.

Moreover, this preliminary analysis permits to rapidly locate the sensitive area for each parameter and take it into account to define the thermocouple location. The analysis is performed for one deposit, and the optimal instrumented areas are proposed. For the welding test as described in Section 2, the specimen was equipped with thermocouples in these optimal areas for several deposits.

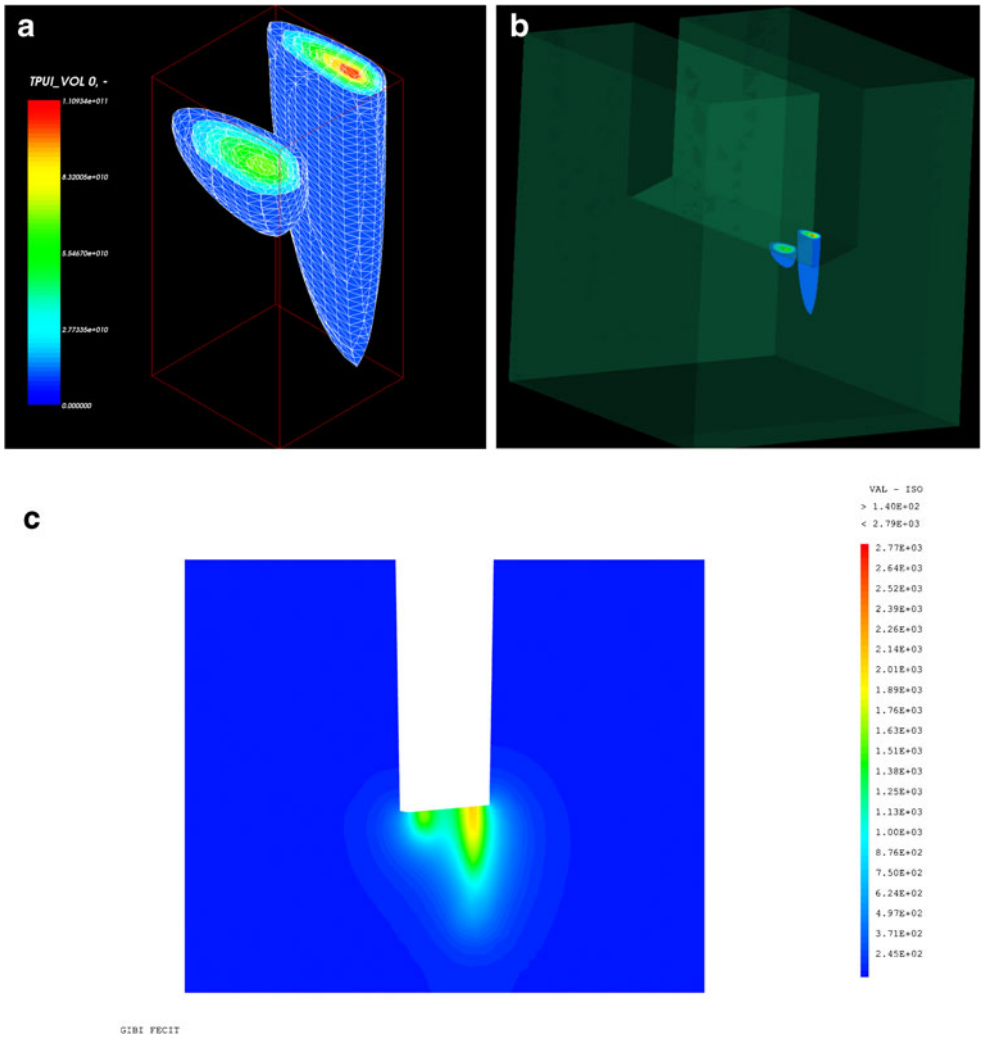

Fig. 6 Energy distribution for a deposit (watts per cubic meter) (**a**) and location in the right side of the groove (**b**). Corresponding thermal field (degree Celsius) (**c**)

3.3 Heat source identification

3.3.1 General characteristics

To identify the heat source parameters, the experimental data are compared with the calculated ones. The observables concern the temperature evolutions in solid zone and the bead shape . For the temperatures, the problem consists in the minimization of the objective function $S(\boldsymbol{\beta})$ described in Eq. 6 [3, 12]:

$$S(\boldsymbol{\beta}) = \sum_{j=1}^{m} \sum_{i=1}^{n} \left(T_{ij} - \tilde{T}_{ij}(\boldsymbol{\beta}) \right)^2 \tag{6}$$

T_{ij} and $\tilde{T}_{ij}$ are, respectively, the measured temperatures and the calculated ones; $\boldsymbol{\beta}$ represents the unknown parameter vector of the heat source model; n and m are the number of thermal sensors and the quantity of temporal measurements, respectively. After optimization, the residues have to be as low as possible. In the case of the bead shape, the objective function is not so easy to find. Usually, people used the width or the penetration depth or both to obtain a scalar value [13]. In the present work, because of the assymmetrical shape of the bead, this criterion are not sufficient to ensure that the bead is well simulated. Then, we have to compare a shape, and, for this purpose, we used a criterion based on the *Hausdorff* distance $h(A, B)$ [14]. This metric measures the distance between two subsets A and B of a metric space (7).

$$h(A, B) = \max\left(d_A(B), d_b(A)\right) \tag{7}$$

where $d_B(A) = \max_{x \in A} d(x, B)$ is the distance between sets B and A, considering $\rho(x, b)$ the *Euclidean* distance between two points x and b; $d(x, b) = \min_{b \in B} \rho(x, b)$ is the distance

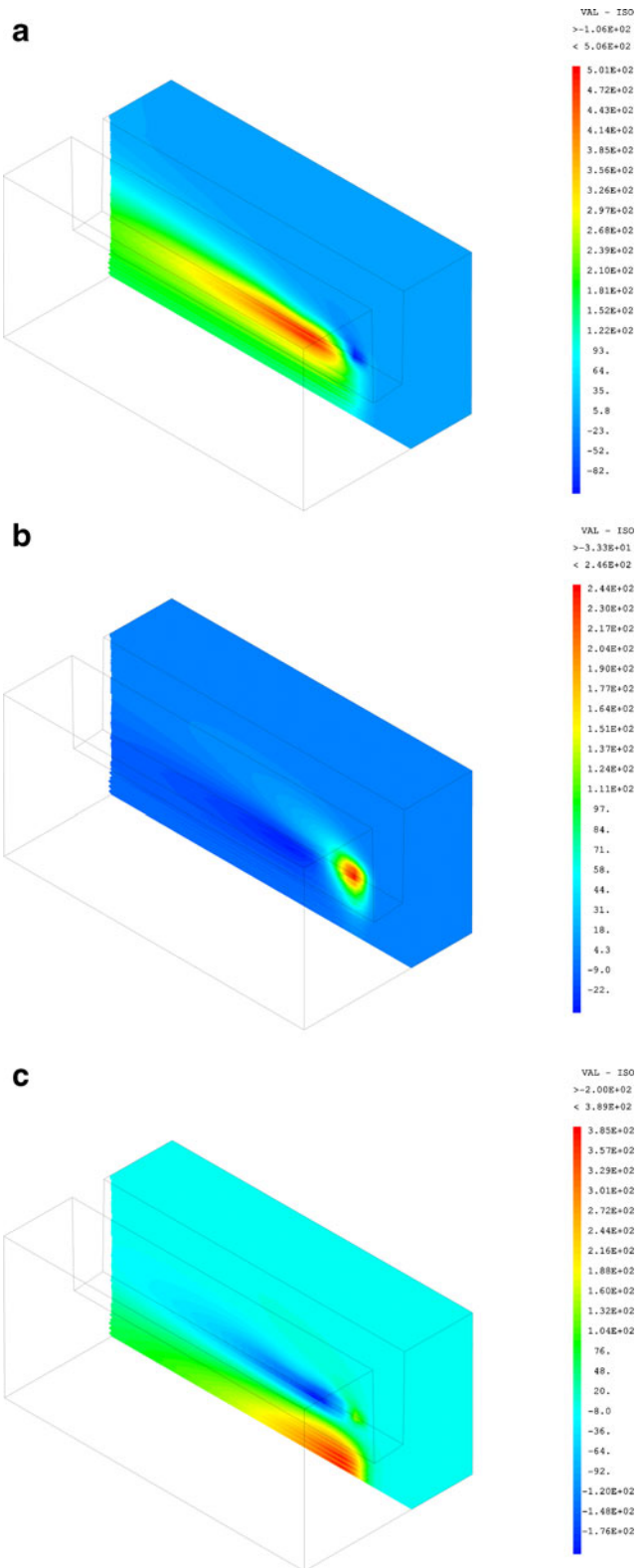

Fig. 7 Reduced sensitivity, on the left part of the groove, of the left *Goldak* heat source parameters: Q (**a**), a (**b**), and b (**c**)

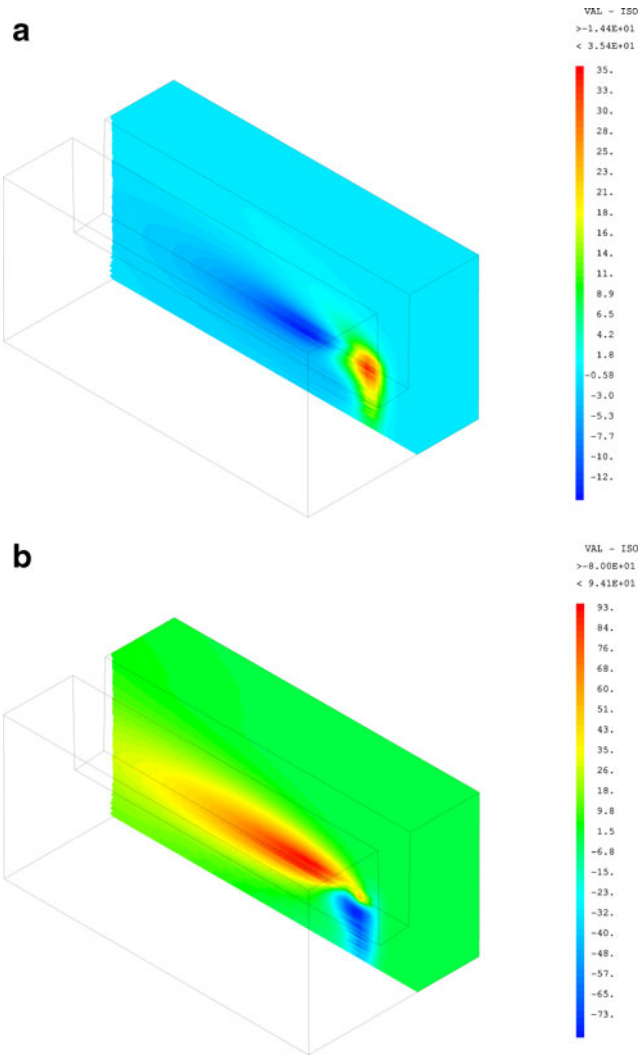

Fig. 8 Reduced sensitivity, on the left part of the groove, of the left *Goldak* heat source parameters: C_f (**a**) and C_r (**b**)

between a point x and a set B; and $d_A(B) = \max_{x \in B} d(x, A)$ is the distance between sets A and B. The minimization is performed in this case with the following objective function (8):

$$S(\boldsymbol{\beta}) = h(A, \tilde{A}(\boldsymbol{\beta}) \tag{8}$$

where A and $\tilde{A}$ describe the experimental and simulated bead shape, and $h(A, \tilde{A}(\boldsymbol{\beta})$ represents the distance between them. In practice, the optimization have been performed both from the temperature data and bead shapes, and the objective function is a linear combination of the two dimensionless criteria applying a weight coefficient α depending on the importance the user wants to give to the thermal

evolutions or to the bead shape. Then the objective function becomes (9) as follows:

$$S(\boldsymbol{\beta}) = (1-\alpha)\frac{\sum_{j=1}^{m}\sum_{i=1}^{n}(T_{ij} - \tilde{T}_{ij}(\boldsymbol{\beta})^2}{m \times n \times T_{\text{ref}}^2} + \alpha\frac{h(A, \tilde{A}(\boldsymbol{\beta})}{\frac{\sqrt{L^2+P^2}}{2}} \tag{9}$$

The dimensionless criteria are obtained from a temperature $T_{\text{ref}} = \frac{T_{\text{liquidus}}}{3}$ for the temperatures and from a distance $\sqrt{L^2+P^2}$ (L is the bead width and P the penetration depth). The minimization resolution consists in calculating the local minimum $\hat{\boldsymbol{\beta}}$ (10):

$$0 = \frac{\partial S(\boldsymbol{\beta})}{\partial \boldsymbol{\beta}}(\hat{\boldsymbol{\beta}}) = 2\left[-\frac{\partial \tilde{Y}^T}{\partial \boldsymbol{\beta}}\right][Y - \tilde{Y}] \tag{10}$$

Writing the *Jacobian* $J = \left[\frac{\partial \tilde{Y}^T}{\partial \boldsymbol{\beta}}\right]^T$, when $\tilde{Y}$ is linear with $\boldsymbol{\beta}$, and $\hat{\boldsymbol{\beta}}$ is obtained by the following relation (11):

$$\hat{\boldsymbol{\beta}} = [J^T J]^{-1} J^T Y \tag{11}$$

The system resolution is made with the L-BFGS algorithm [15].

3.3.2 Results and discussions

The initial value of the vector $\boldsymbol{\beta}$ is defined a priori before optimization. For the present configuration with two *Goldak* volumetric sources, the vector consists in ten parameters (five parameters for each model). For thermocouples, only those which have exceeded 300 °C are selected, which leads to consider nine thermocouples for the 13th deposit. After optimization, the values of the parameters which have led to the best fit are retained for the heat thermal source. Different types of criterion have been used, considering only temperatures, only bead shape, or both. Finally, the best results are obtained when considering the mixed objective function with a more important weight applied to the bead shape data (with $\alpha = 0.4$ in Eq. 9 [16]).

Considering only temperatures, if the calculated temperature evolutions for the considered thermocouples in solid area are satisfactory with respect to the experience, the bead shape is absolutely not representative. The size of the weld pool remains too small.

When the optimization is made from the bead shape, only this one is close to the experimental geometry, but calculated temperatures in the specimen do not fit at all. The simulated temperatures overestimate the measured ones. This result is quite surprising: if the weld pool boundary is correct, then the temperature field outside this region should also be correct [17, 18].

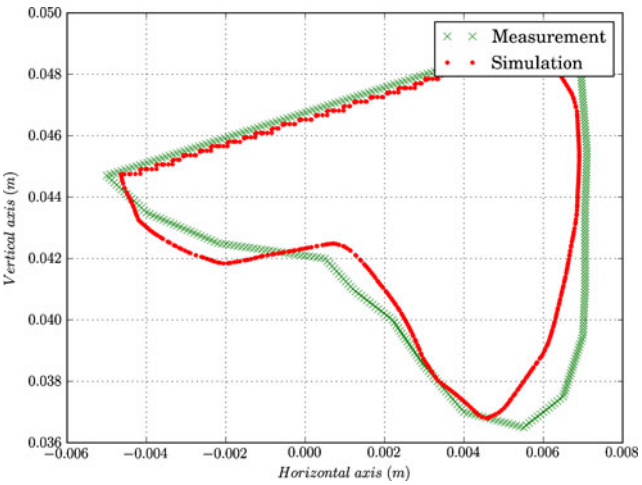

Fig. 9 Bead shape (axes in meter) comparison between experimental (*green cross*) and calculated observables (*red points*) after optimization for deposit 13

When considering bead shape and thermocouples, the optimization for the deposit 13 leads to appropriate results in terms of the bead shape (Fig. 9) and the temperature evolutions (Fig. 10). The model produces a representative bead shape despite its complexity. Temperature gradients in the solid area are also very satisfactory even for an important number of thermocouples located in more or less distant regions from the deposit. Nevertheless, the temperatures are all slightly overestimated. The more important difference

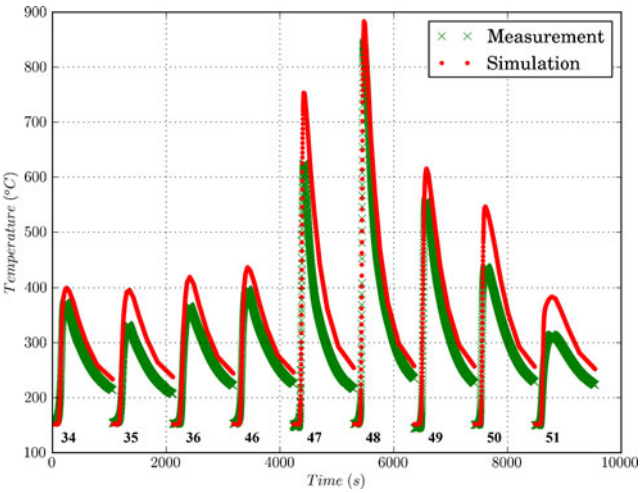

Fig. 10 Temperature comparisons between experimental (*green cross*) and calculated observables (*red points*) after optimization for deposit 13, thermocouple channels 34, 35, 36, 46, 47, 48, 49, 50, and 51

for the thermocouple on channel 47 is probably mostly due also to an error on the experimental position because this thermal sensor always exhibits a particular behavior after the various optimizations which have been performed for the other passes.

In order to obtain a good fit of the bead shape, the calibration implies to apply a too important energy parameter Q for the *Goldak* model on the right side especially to get the penetration depth. As a result, this explains the overestimated values for the calculated peak temperatures. This result has also been found with similar calibration results for other deposits in the groove. As a result, the limit of the conduction model is achieved for this kind of welding configuration. In order to obtain the best fit, several solutions could be considered: by decreasing the latent heat of fusion, less energy will be needed to melt the metal; and by decreasing the conductivity in the weld pool and increasing it in the solid region. Another solution to consider is latent heat of fusion and conductivity as unknown parameters in the heat source calibration process as was preliminary made by Debroy [19].

4 Conclusions

The main objective of this work was to identify by inverse method a 3D thermal model for a deep narrow groove multipass GMAW process configuration for low-carbon steel. The methodology is based on an experimental and numerical approach. The experimental data participate to the establishment of the numerical model, and thus, the more accurate they are, the more the model is relevant. For this project, we developed very specific and accurate methodology for obtaining experimental welding data (temperatures and bead shape). The optimization based on a heat conduction model allows achieving relevant bead shape and temperatures in the solid zone for the narrow gap GMAW multipass welding on 16MND5 ferritic steel thick plate. The values of the ten parameters for the two volumetric sources which have been obtained after optimization are retained for the heat source model. It can be used as thermal loading for subsequent thermal metallurgical mechanical calculations. It is obvious that the limits of the heat conduction model have been reached. It is the reason why the identification of the heat source to obtain satisfactory results for this welding configuration required the use of two volumetric sources, which increases in addition to the number of unknown parameters. So to complete this work, we propose to improve the inversed model by taking into account physical phenomena in the weld pool to describe the convention movements. Considering a fluid flow model, it will be probably easier to obtain the complex bead shape than with the conduction model, and the heat source model will be simplified, containing fewer parameters to be identified.

References

1. Goldak JA, Chakravarti A, Bibby M (1984) A new finite element model for welding heat source. Metall Trans B 15B:299–305
2. Emery AF, Nenarokomov AV (1998) Optimal experiment design. Meas Sci Technol 9(6):864
3. Beck JV, Arnold KJ (1977) Parameter estimation in engineering and science. Wiley, New York
4. Asserin O (2009) Methodology for heat source parameters identification in the frame of computational weld mechanic. Implementation with the software WPROCESS. Technical report DEN/DANS/DM2S/SEMT/LTA/09-003/A, CEA
5. Wang HX, Sun JS, Wei YH, Zheng YY (2005) Simulation of GMAW thermal process based on string heat source model. Sci Technol Weld Join 10(5):511–520
6. Nagesh D, Datta G (2008) Modeling of fillet welded joint of GMAW process: integrated approach using doe, ann and ga. Int J Interact Des Manuf (IJIDeM) 2(3):127–136
7. Hu J, Tsai HL (2008) Modelling of transport phenomena in 3D GMAW of thick metals with V groove. J Phys D Appl Phys 41(6):065202
8. Schnick M, Fuessel U, Hertel M, Haessler M, Spille-Kohoff A, Murphy AB (2010) Modelling of gas-metal arc welding taking into account metal vapour. J Phys D Appl Phys 43(43):434008
9. Roatta JL (2004) Heat source modelling for the accurate simulation of the temperature field in a 316L narrow gap multi-pass arc welding. Master Thesis, University of Nantes
10. Gabriel F, Ayrault D, Fontes A, Roatta JL, Raynaud M (2007) Global method for estimation of heat source parameters dedicated to narrow gap GTA welding. In: Cerjak H, Bhadeshia HKD, Kozeschnik E (eds) Mathematical modeling of weld phenomena, vol 8. TU Graz, Verlag der Technischen Universität Graz, Graz, pp 25–27
11. Azar AS, Ås SK, Akselsen OM (2012) Determination of welding heat source parameters from actual bead shape. Comput Mater Sci 54(0):176–182
12. Özişik MN, Orlande HRB (2000) Inverse heat transfer: a fundamentals and applications. Taylor & Francis, New York
13. Kumar A, DebRoy T (2004) Guaranteed fillet weld geometry from heat transfer model and multivariable optimization. Int J Heat Mass Transfer 47(26):5793–5806
14. Huttenlocher DP, Klanderman GA, Rucklidge WJ (1993) Comparing images using the Hausdorff distance. IEEE Trans Pattern Anal Mach Intell 15:850–863
15. Nocedal J (1980) Updating quasi-Newton matrices with limited storage. Math Comput 35:773–781
16. Asserin O, Ayrault D (2011) Heat source identification for narrow gap gaz metal arc welding. Technical report DEN/DANS/DM2S/SEMT/LTA/11-014/A, CEA
17. Lindgren LE (2007) Computational welding mechanics: thermomechanical and microstructural simulations. Woodhead Publishing in Materials, Cambridge
18. Lundbäck A, Alberg H, Henriksson P (2005) Simulation and validation of TIG welding and post weld heat treatment of an Inconel 718 plate. In: Cerjak H et al (eds) Mathematical modelling of weld phenomena, vol 7. Technischen Universität Graz, Verlag der Technischen Universität Graz, Graz, pp 683–696
19. De A, DebRoy T (2004) Probing unknown welding parameters from convective heat transfer calculation and multivariable optimization. J Phys D Appl Phys 37(1):140